ISSN: 2692-5397
DOI: 10.33552/MCMS.2022.04.000596
Modern Concepts in Material Science
Iris Publishers

Research Article

The Impact of Simulated Direct Sun Radiation on the Thermal and Optical Performance of Cellular Glass Coated with WO_3 Based Painting

Corina Macarie[1], Stefan Danica Novaconi[1], Florina Stefania Rus[1]* and Madalina Ivanovici[1,2]*

[1]*National Institute for Research and Development in Electrochemistry and Condensed Matter, Romania*

[2]*Politehnica University of Timisoara, Romania*

***Corresponding author:** Florina Stefania Rus National Institute for Research and Development in Electrochemistry and Condensed Matter, Aurel Paunescu Podeanu Street, No. 144, 300569 Timisoara, Romania and Madalina Ivanovici, National Institute for Research and Development in Electrochemistry and Condensed Matter, Aurel Paunescu Podeanu Street, No. 144, 300569 Timisoara, Romania, Politehnica University of Timisoara, Piata Victoriei, No. 2, 300006 Timisoara, Romania.

Received Date: June 24, 2022

Published Date: July 08, 2022

Abstract

The thermal and optical properties of commercial glass foam covered with a functional coating designed for exterior and environmental applications were investigated. The coating was prepared using WO_3 a photocatalytic material - as a pigment and acrylic resin - as a binder. The temperature variation at different depth points and on the surface of the glass foam, before and after the application of 1-4 layers of WO_3, during the exposure to the simulated sunlight, was monitored. Physical and chemical characterization - RGB and reflectance measurements were conducted for the glass foam surface before and after being covered with WO_3-based coating and FT-IR, Raman and EDAX spectroscopy, X-ray diffraction, and 3D laser scanning microscopy were used for the as-prepared WO_3 powder, the glass foam, and the applied layers of WO_3 based coating. The change in WO_3-based coating spectral properties under external stimuli was emphasized and correlated with the optical and structural properties of the WO_3 powder. Surface roughness, color, and spectral reflectance were improved after multiple layers of the coating.

Keywords: WO_3 pigment; Color change; Glass foam; Direct simulated solar irradiation; Spectral reflectance

Introduction

Glass foam belongs to new generation materials, designed, among other applications, especially as a heat insulator in the building industry. Furthermore, it is considered an ecological and efficient insulation material given the fact that it is being developed both commercially and in the research field from glass waste resources presenting multiple properties of interest (chemical, physical and biological stability, excellent insulating properties, lightweight, fire and water resistance, etc.).

Based on its properties and commercial applications, glass foam, also known as cellular glass, can be used as an insulator for roofs, building facades, sub-base (gravel) and industrial piping and installation. Among the chemical and physical properties intensively studied, there mentioned porosity, thermal conductivity, density, sound insulating properties, thermal resistance, and compressive strength, concerning the properties of efficient and long-lasting insulating materials. Nevertheless, based on the current scientific

literature, limited experimental studies have involved investigating the glass foam thermal response as a part of an insulating system for building applications [1-6]. Building energy consumption for heating, cooling, and lighting has been one of the most important sectors in global energy consumption. Smart windows, which can change their optical and thermal properties on the fly, are seen as a promising technology for reducing energy consumption in buildings. Also, in the context of the necessity of developing smart systems in the construction field as a research trend related to air pollution reduction is to be mentioned the application of exterior photocatalytic coatings that involves the use of photocatalytic compounds as pigments. As reported in the literature, paints using titanium oxide and zinc oxide as pigments because to their photocatalytic properties were studied as potential coatings for reducing air pollutants such as nitrogen oxides and volatile organic compounds from the atmosphere [7,8]. As well, WO_3 a visible-light active photocatalytic material reported to be used as a pigment in ceramics, cosmetic products and for nano inks. Because of its low toxicity and outstanding biocompatibility with human, animal, and plant cells, tungsten oxide is one of the most popular inorganic nanomaterials [9]. Because of its wide range of continuously adjustable optical properties, excellent reversibility, low energy consumption, high coloration efficiency, and environmental friendliness, tungsten oxide (WO_3) has been regarded as the most promising electrochromic materials [10-15]. WO_3 possesses a series of properties (catalytic, photocatalytic, chromophoric, semiconductor properties) that make it appealing in fields such as photocatalysis dedicated to pollution reduction and energy production, sensors, electrochromic and photochromic smart windows also an efficient electrocatalyst for hydrogen evolution in acidic water [16-20]. As a result, one of the research priorities was to improve the properties of WO_3 materials for use in reducing building energy consumption and greenhouse gas emissions for a significant recovery of total energy consumption and a reduction of CO_2 emissions in both developed and developing countries worldwide where the problems of resource depletion and pollution have been a growing topic of worry. In this study, commercial glass foam covered with water-based coating prepared using WO_3 as a pigment was investigated as an environmentally friendly insulation system manifesting multiple properties. This study investigated the thermal and optical behavior of glass foam covered with a new coating containing pigment with photocatalytic and photochromic properties. The approach of the study consisted of analyzing the thermal behavior of the uncovered and covered glass foam with WO_3-based painting and optical properties changes of the coating obtained as a response to simulated solar direct radiation exposure in specific conditions, and further discussed as separate matters, attended by structural, compositional, and textural characterization of the glass foam, WO_3 pigment and WO_3-based coating. To the best of our knowledge, no studies were reported for preparation and optical characterization of acrylic WO_3-based painting applied on an insulating material for the construction field. The based coating was prepared using three main components: WO_3 as a pigment - a material largely studied for its photocatalytic activity in the visible-light spectrum, chemical stability, earth abundance and its potential use in the environmental applications, acrylic resin as binder suitable for both interior and exterior finishing coatings, known for good oxidative, UV stability, resistant to breakage and high temperature, good adhesion to non-porous and porous surface, elasticity and widely used for the preparation of emulsion paints and water as a solvent - a cheap, abundant and nontoxic resource [17,18,21-23].

Experimental part

The complex material studied in this work was commercial glass foam (Pinosklo from Iridexplastic SRL company). The main chemical-physical properties of glass foam are as follows: density: 110 - 160 kg/m^3, thermal conductivity: 0.045 - 0.054 W/m • K, reaction to fire class A1, compression strength: 700 kPa, bending strength of 500 kPa, capillary water absorption: 0.5 kg/m^2. Glass foam pieces 10 cm long, 10 cm wide, and 4 cm deep were cut to be covered with WO_3 pigment previously obtained.

Preparation of the WO_3-based coating

Firstly, the WO_3 pigment was obtained from tungstic acid (pure H_2WO_4 procured from Riedel-de Haën AG) by thermal treatment. The tungstic acid was heated at 600°C for 6 h in air atmosphere, in which the dehydration process occurred so that internal water molecules of the tungstic acid were removed, as presented in (1) as in the study described by Nogueira et All [24].

$$H_2WO_4 \rightarrow WO_3 + H_2O \quad (1)$$

The obtained WO_3 pigment and acrylic resin (from Craft Concept S.R.L) were mixed in a weight ratio of 1:1 (each counting for 35 wt% of the total mixture) and the amount of water added was adjusted so that the coating can be easily applied by brushing. The synthetic method proposed allows for the scalable preparation of highly efficient low-cost WO_3-based photochromic materials.

FT-IR, Raman, EDAX spectroscopy, and X-Ray diffraction

FT-IR and Raman spectroscopy were used as characterization techniques for the commercial glass foam and synthesized WO_3 powder to identify the main functional groups of their chemical composition. Moreover, to provide a more detailed investigation about the chemical composition of the commercial glass foam, EDAX spectroscopy was selected for elemental analysis. FT-IR characterization was performed using FT-IR spectrometer Vertex 70 (Bruker, Germany) using the KBr pellet method in the wavenumber range of 400-4000 cm^{-1} cm^{-1}, 128 scans and a resolution of 8 cm^{-1}.

Raman spectra were obtained using a scanning probe microscopy system: Multi Probe Imaging -Multi View 1000TM system (Nanonics Imaging, Israel) and the crystalline phase of the WO_3 powder was investigated using PANalyticalX'Pert Pro MPD-type diffractometer with Cu-Kα radiation (λCu =1.54060 Å) and a 2θ-step of 0.016, from 20° to 80°. Elemental mapping of the commercial glass foam was accomplished using Inspect S PANalytical SEM/EDX.

Optical characterization and surface morphology investigation of the WO_3-based coating glass foam

Optical properties (RGB and spectral reflectance) were investigated for the glass foam and of the WO_3-based coating applied on the glass foam. The reflectance and RGB measurements provide additional information regarding the color stability of the coating and the changes of the optical response influenced by the application of multiple layers.

The RGB measurements consisted of monitoring the proportion of each primary color (red, green, and blue), which allows to simulate the color of the investigated surfaces. The color analyses were conducted (with a color Meter-PCE-RGB 2 from PCE Instruments UK Ltd) on the uncovered glass foam and on the coating, layers applied on the glass foam before and after the system was exposed to the direct simulated solar light.

The reflectance was measured on the uncoated glass foam and on the applied layers of the coating before the thermal experiments. The reflectance analysis was accomplished by an integrating sphere of 50 mm (model ISP-50-8-R-GT from Ocean Optics) connected to a Jaz modular UV-VIS spectrophotometer (procured from Ocean Optics) and a light source (LS-1 from Ocean Optics) with applied of a reference correction.

The surface texture of the layers of WO_3-based coating was analyzed compared with the uncoated glass foam using 3D laser scanning microscopy. Therefore, the images of the surfaces were obtained using 3D laser scanning microscope OLS 4000 Lext Olympus.

Thermal investigation

The thermal properties of the glass foam covered with WO_3-based coating system were analyzed by simulating real conditions for which this system can be used as an external insulating layer of the building envelope. The commercial glass foam, Pinosklo cellular glass, was cut into pieces of the following sizes: 10 cm × 10 cm × 4 cm (length × depth × height) and subjected to the experimental investigations. Each piece was fixed in a polystyrene box so that the heat transfer between the exterior and interior does not occur on the sideways. The upper surface of the samples was exposed to the heating source - simulated solar radiation (provided by Sol2A 94042A, Oriel Instruments/Newport Corporation) and the bottom surface was placed on a stainless-steel surface. The ambient temperature was maintained constant at 23°C.

For two hours, the temperature was measured at the surface of the sample with an infrared camera (Fluke Ti110 thermal imaging camera) and at certain points inside the sample situated at equal distances across the sample height using type K thermocouples connected to a thermometer with 4 channels (model TM –946 from Lutron Electronic). Temperature measurements were conducted for glass foam samples before and after applying each layer of WO_3-based coating. Four layers of WO_3-based coating was applied on the glass foam and the irradiance of the simulated solar radiation at the surface of the sample was around 895 W/m^2 in the visible domain and 10 W/m^2 for UV domain.

Results and Discussion

Spectroscopic characterization of WO_3 powder WO_3-based coatings and commercial glass foam

The FT-IR spectra (Figure 1a) of the WO_3 powder reveal two peaks associated with the adsorbed water molecules at ~3459 cm^{-1} and ~1640 cm^{-1} ascribed to the stretching vibration - ν(O-H) and, respectively, to the bending vibration mode δ(H-O-H). The broad peak situated at 840 cm^{-1} can be attributed to the ν(W-O-W) vibration with a shoulder present at 776 cm^{-1}, which can be assigned to the ν(O-W-O) vibrations [12,13].

Additional vibrational modes for WO_3 powder are identified in the Raman spectra (inset of the Figure 1b) between 50 cm^{-1} and 1000 cm^{-1} at 720, 812, 332, and 278 cm^{-1}. As reported in the study [25], the revealed bands of the WO_3 Raman spectra correspond to the crystalline monoclinic tungsten trioxide (m- WO_3).

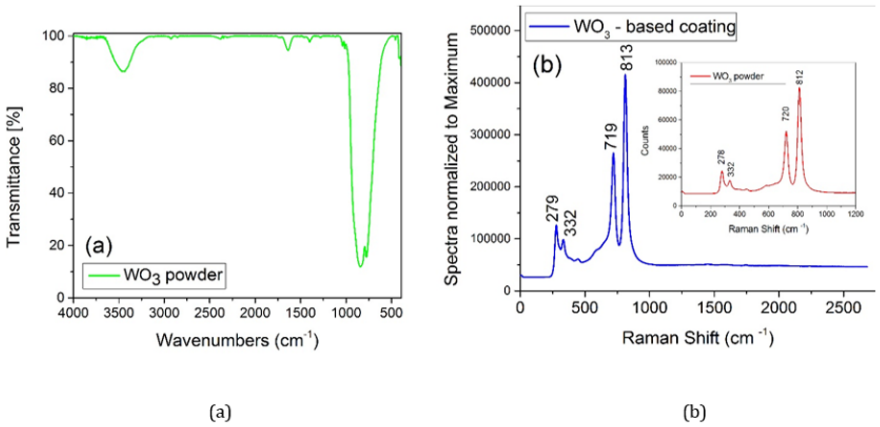

(a) (b)

Figure 1: a) FT-IR spectra of WO_3 powder and (b) Raman spectra of WO_3-based coatings with inset of Raman spectra for WO_3 powder.

Therefore, the peaks found at 720 cm^{-1} and 812 cm^{-1} are ascribed to the stretching vibration mode (ν(O-W-O)) and the peaks situated at 278 cm^{-1} and respectively 332 cm^{-1} can be attributed to the bending vibration mode O-W-O of bridging oxygen [25-27]. The same Raman bands were present also in the Raman spectra of the WO_3-based coating and no other peaks were identified, suggesting a good distribution of the pigment in the coating layer.

The purity and crystalline phase of the synthesized WO_3 were further investigated using X-ray diffraction spectroscopy. The XRD pattern (Figure 2) shows diffraction peaks that are ascribed entirely 100% to the monoclinic crystalline structure of WO_3 with the lattice parameters of a=b = c=5.078 Å as confirmed by the standard card (JCPDS: 75-2072) using Rietveld refinement analysis, reflecting the high purity of the crystalline phase.

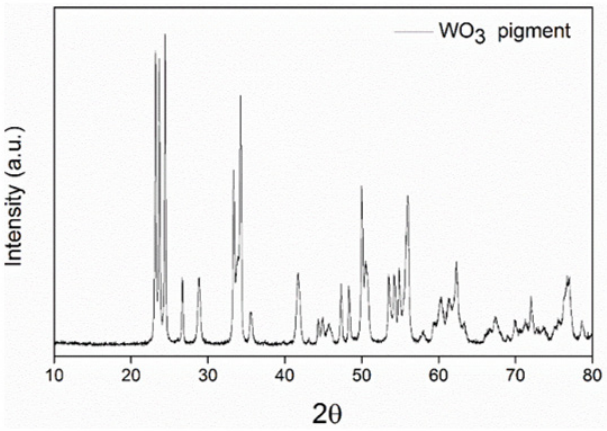

Figure 2: Powder XRD diagram of WO_3 pigment.

Based on the information provided by XRD analysis, the structural parameters of the WO_3 powder are presented in table 1. The sharp peaks at 2d=23.18, 23.63, 24.38, 26.7, 28.94, 33.38, 34.26, 35.44, 41.74, 47.27, 48.25, 49.99, 53.46, 54.23, 54.88, 55.95, 76.8 correspond to the planes (002), (020), (202), (120), (112), (021), (202), (220), (221), (002), (040), (400), (022),(202), (240), (401), (422) [28,29] (Table 1).

The crystallite sizes were determined from X-ray diffraction line broadening using the Debye-Scherrer equation (Equation 2) for calculating particle size:

$$D = \frac{K\lambda}{\beta \cos\theta} \quad (2)$$

Table 1: Structural parameters of WO_3 powder.

Formula $W_{6,00}O_{2,00}$	a [Å] - 5,078(2)
100% WO_3	b [Å] - 5,078(2)
Spatial group P m –3 n (223)	c [Å] - 5,078(2)
The molar mass [g/mol]- 1135,0990	α [degree] - 90
Calculated density [g/cm^3] - 14,3895	β [degree] - 90
V (106 pm^3) - 130,97100	γ [degree] - 90

Where: D is the mean size of crystallites (nm), K is the Scherrer constant, λ is wavelength of the X-ray beam used (1.54, 184 Å), β is the Full width at half maximum (FWHM) of the peak and θ is the Bragg angle. The calculated crystallite sizes were 68.8 nm.

As widely studied, it must be mentioned that the properties of WO_3, including but not limited to the crystal phase, surface chemistry, and band gap, that are likewise interdependent properties, have a strong impact further in their application, such as photocatalysis, chromism and semi conductivity [17,18]. In Nagy et all study [18], it has been pointed out that WO_3 powders of different crystal phases (m- WO_3, h- WO_3, o- $WO_3 \cdot 0.33H_2O$, and its combinations) and morphologies (nanorods, cuboidal nanoplates, nanowires, etc.) led to different values of band gaps and distinct appearance (yellow or blue). The variations in WO_3 powder structural and morphological properties also involved different photocatalytic performances. In other experimental studies [30,31] it has been reported that the enhanced photocatalytic activity was obtained for m- WO_3 compared to h- WO_3 and, respectively, for o- WO_3/Al-W compared to c- WO_3/Al-W. Similarly, it was illustrated that photochromic activity is affected by the crystal phase of WO_3 therefore, hexagonal phase of WO_3 showed better photochromic properties than the cubic phase [32].

Similar to the FT-IR spectrum of WO_3, in the FT-IR spectra of the glass foam (Figure 3a), the bands at 3448 cm^{-1} and 1625 cm^{-1} correspond to the vibrations of water groups. As is specified on the producer site, the commercial glass is produced from recycled materials (such as container and window glass), whereas the carbon black is used as the foaming agent. Most common glasses used for the production of containers and windows are soda-lime glass and potash glass. The main constituent oxides of these types of glasses are SiO_2, CaO, Na_2O, K_2O, of which SiO_2 represents the major component (>50%-wt%) [33-35].

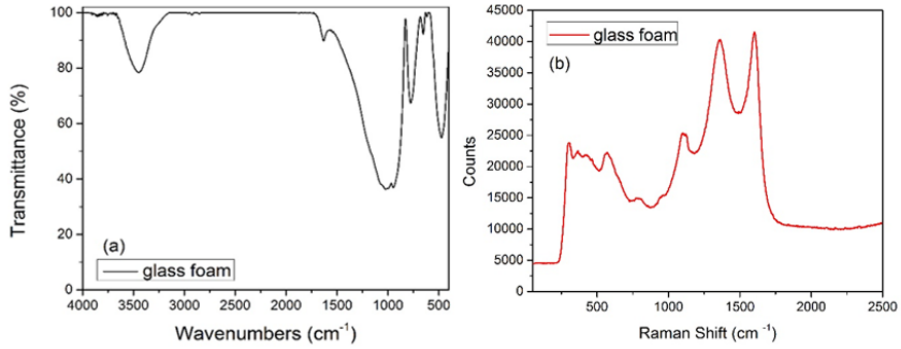

Figure 3: FT-IR (a) and Raman (b) spectra of the commercial glass foam.

The peaks revealed in the FT-IR spectra of the commercial glass foam correspond to the vibrations of SiO_2 as further presented the broad band at 1022 cm^{-1} may be ascribed to the Si-O-Si anti-symmetric stretching of bridging oxygen within the tetrahedral and the weak peak at 920-980 cm^{-1} can be ascribed to Si-O- stretching with nonbridging oxygens. The bands at 770 cm^{-1} and 475 cm^{-1} can be attributed to the Si-O-Si symmetric stretching vibrations of the bridging oxygens and to the bending modes of Si-O-Si and O-Si-O, respectively [23].

In the Raman spectra (Figure 3b) of the glass foam, two intense bands are observed at 1606 cm^{-1} and 1359 cm^{-1} that correspond to the carbon element used as the foaming agent, explaining the black of the glass foam. Also, the peak at 1107 cm^{-1} is characteristic of silica tetrahedra with one non-bridging oxygens. The bands between 300 cm^{-1} and 600 cm^{-1} are very likely to correspond to the vibration of oxygen atoms in Si-O bonds but can also be attributed to M-O-M groups, where M can represent Si and other elements [36,37]. Based on the EDAX analysis, the investigation of the elemental composition for commercial glass foam is more detailed via semi-quantitative analysis. EDAX spectra (Figure 4) attest the oxygen as the major element followed by silicon given by the silicon dioxide-the main component of the glass foam, as previously mentioned. The other elements revealed here are Na (11.51 wt%), Ca (5.68 wt%), Mg (1.91 wt%) and Al (1.29 wt%).

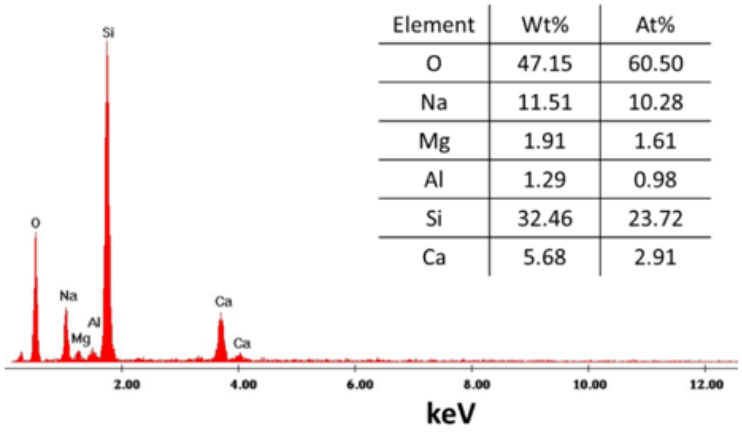

Element	Wt%	At%
O	47.15	60.50
Na	11.51	10.28
Mg	1.91	1.61
Al	1.29	0.98
Si	32.46	23.72
Ca	5.68	2.91

Figure 4: EDAX elemental analysis of the commercial glass foam.

Optical characterization and surface morphology investigation of the glass foam and WO_3-based coating

The optical properties in terms of spectral reflectance (diffuse reflection) and color, investigated using the RGB model, were evaluated for the uncovered glass foam sample compared with the glass foam sample after applying every layer of the WO_3- based coating.

As presented in figure 5, the reflectance curve indicates that the maximum reflectance values for layers 1–4 was found in the wavelength range of 480÷580 nm. This domain corresponds mainly to the green wavelength spectrum and to a wavelength spectrum that is attributed to cyan and yellow [38]. The reflectance curve for the uncoated glass foam is nearly uniform across the spectrum between 400 and 700 nm, suggesting the dark gray of the glass foam. The reflection increases from 25.6% to 47% for layers 1-4, indicating a more intense color of the coating and a more proper covering of the coating on the glass foam.

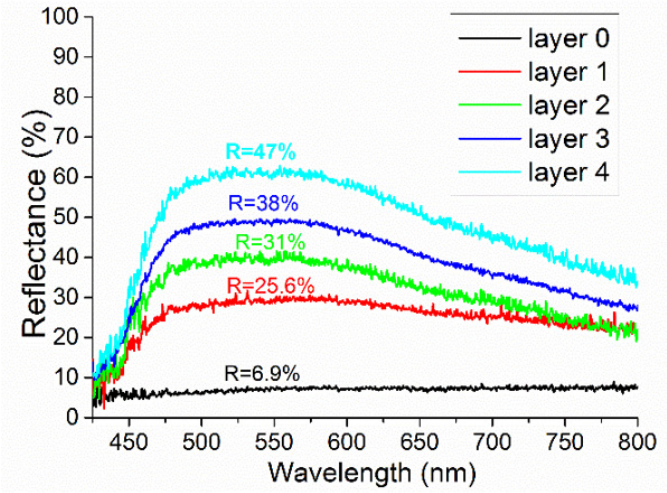

Figure 5: The reflectance of layer 1, layer 2, layer 3 and layer 4 of WO_3-based coating applied on the glass foam compared to glass foam with no coating applied (layer 0).

The yellow-green color of the coating, characteristic of the WO_3 compound, underwent significant changes after being exposed to simulated solar radiation (Figure 6). The color change after exposure to simulated light, investigated using the RGB model, is indicated by a decrease in R, G, B values with approximately 30-40 units for each layer applied, which decreases the strength of the color.

Moreover, the green-yellow color, more clearly noticed for layer 4, as illustrated in figure 7, turns into a green bluish color. This information is also revealed by comparing the proportion of each primary color before and after exposure to simulated solar light. Before irradiation, values attributed to R and G are almost equal and the proportion of B is lower compared to R and G. After irradiation, the proportion of R decreases compared with G, being very similar to B and the proportion of B in relation to G increases compared to the results obtained before irradiation.

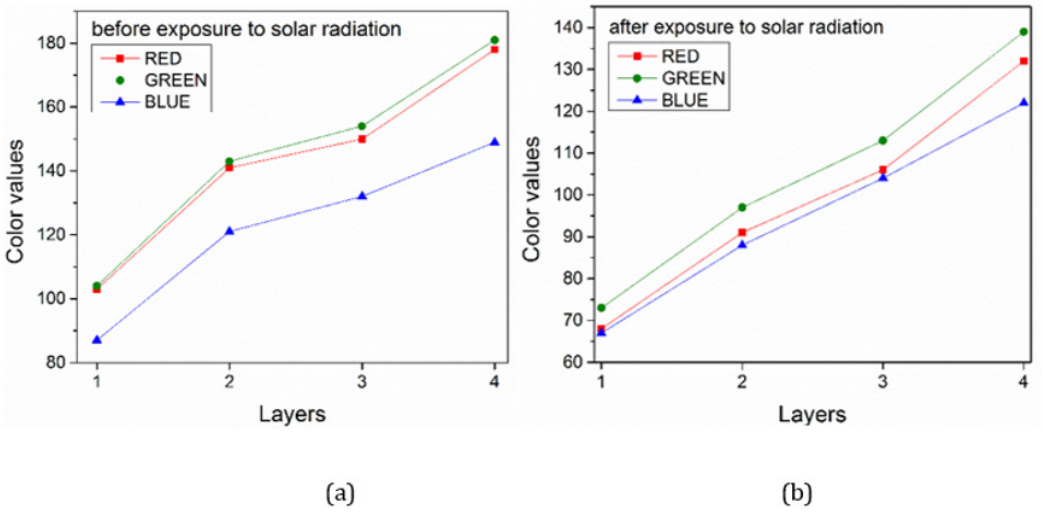

Figure 6: Modification of RGB values (expressed from 0 to 255) for each layer of applied WO_3-coating (a) before and (b) after exposure to simulated solar light.

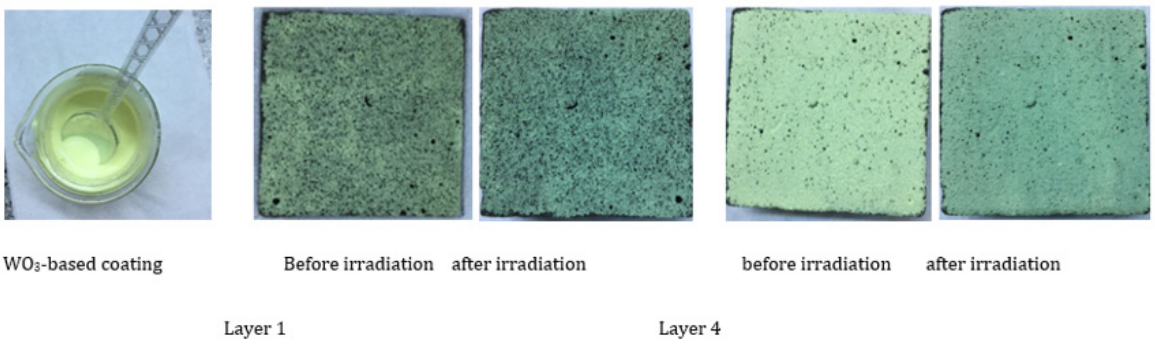

Figure 7: The photos of WO_3-based coating (left side) and of the glass foam covered with of WO_3-based coating (layer 1 and layer 4) before and after solar irradiation.

According to the scientific literature, the chromogenic properties of WO_3 are well known and can be manifested because of photochromism, electrochromism, thermochromism and gasochromism phenomena. In this work, the color change of the coating may be explained by the photoreaction of WO_3 occurring during the exposure to simulated solar light. In the photochromic process, the electron (e^-) and hole (h^+) pairs in the WO_3 are generated due to light irradiation. The former enters the conduction band of WO_3 and the holes react with water from the system, forming Hx WO_3 (equation 3), resulting in a color change in the spectral range from yellow to blue [17,32,39-41].

$$WO_3 + xH^+ + xe^- \rightarrow H_xWO_3 \quad (3)$$

As previously mentioned, WO_3 is a semiconductor with a large applicability spectrum for which the color depends on the oxidation state of the tungsten atoms in the crystal structure. Therefore, the capacity of the powder capturing photons, that is, the amount of photon induced electron-hole pairs directly influence the photochromic properties of the WO_3 compound [8,19].

The glass foam has a porous structure and for this reason multiple layers of the coating were required to achieve an enhanced coverage. Four layers, as previously mentioned, were involved in the study.

In figure 8, it is shown that a more homogeneous dispersion of the coating is achieved as the number of layers increases, which decreased surface roughness (Sq) from 31.45 µm to 17.28 µm and to the decrease of maximum valley depth (Sv) from 640 µm to 285 µm. Based on the 3D images, it can be seen that the coating layering is free of cracks and although the rugosity of the glass foam was lessened after multiple layers, the porous texture, marked by the presence of pores, was maintained for all layers from 1 to 4.

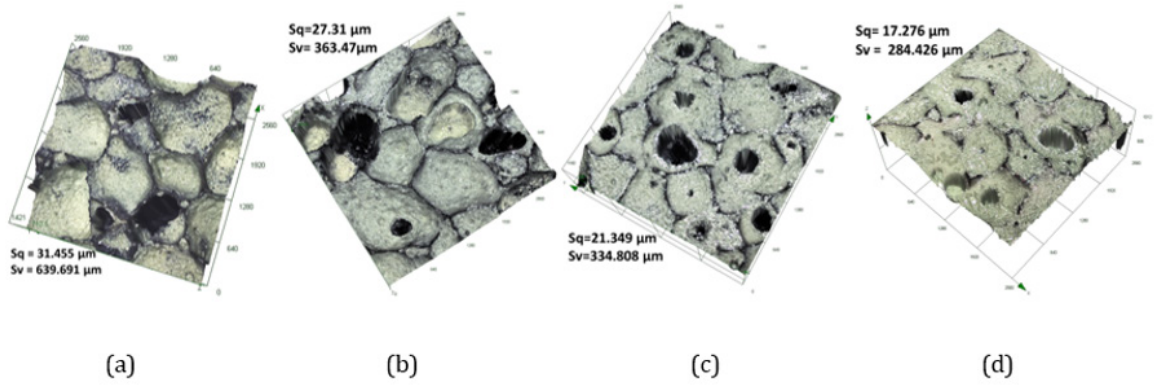

Figure 8: 3D images (5x magnification) for the porous surface of the glass foam covered with (a) layer 1, (b) layer 2, (c) layer 3 and (d) layer 4 of WO_3-based coating.

Thermal behavior evaluation of the glass foams

In figure 9, presents the thermal behavior of the glass foam sample before and after being covered with WO_3-based coating obtained under specific experimental conditions: exposure to simulated solar radiation and constant ambient temperature.

Therefore, in the first step, when no coating was applied, it can be noticed that during the radiation exposure, the temperature of the surface (Tsupr) and the temperature measured at the four points across the glass foam sample height (T1, T2, T3, T4) increased rapidly from approximately 27°C and respectively 24°C (for T1, T2, T3, T4) to ~ 78-80°C and respectively 74°C, 64°C, 51°C, 41°C after 20 min, followed by temperature stabilization specified by a plateau value in the range between 20 and 120 min for all five monitored zones.

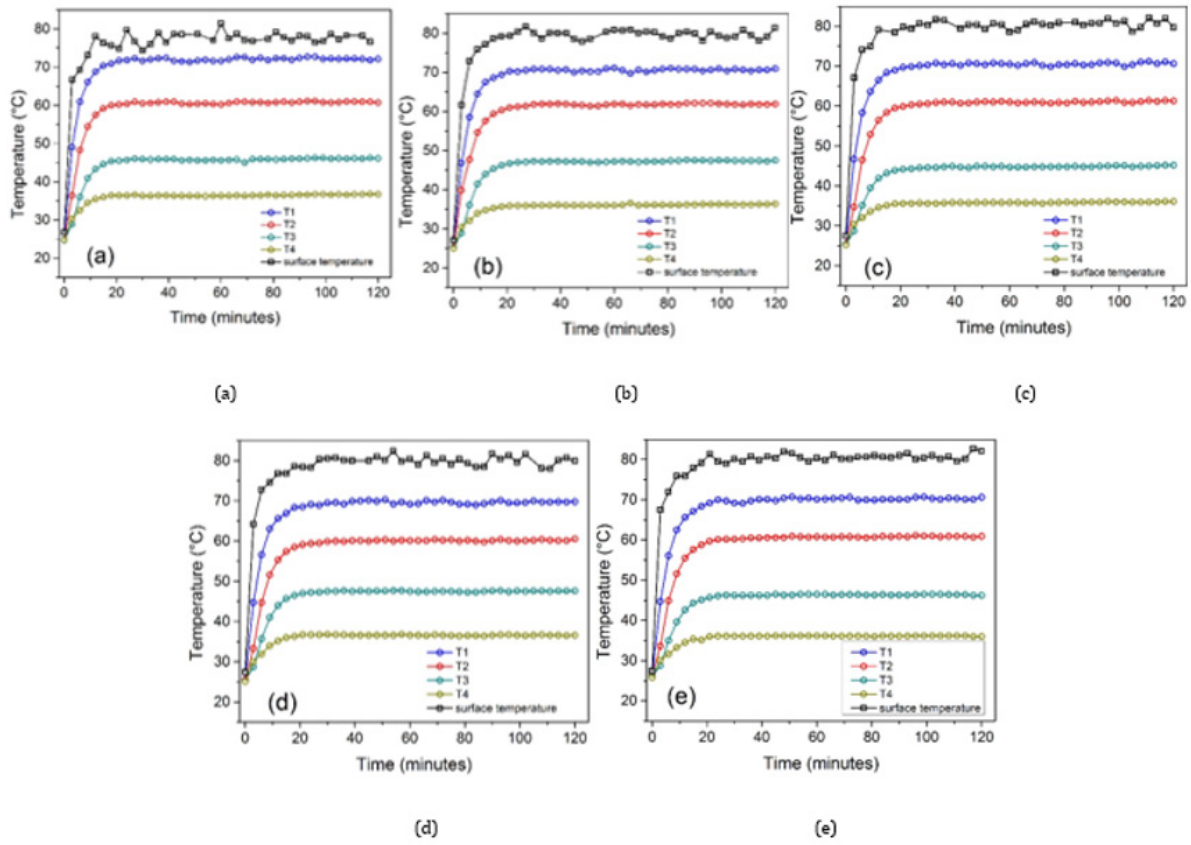

Figure 8: Thermal response of the uncoated glass foam (a) and of the glass foam covered with WO_3-based coating ((b) – layer 1; (c) – layer 2; (d) – layer 3; (e) – layer 4)) during the exposure to simulated solar radiation.

The temperature values inside the glass foam sample decreased constantly from one measuring zone to the following one as the heat of the solar radiation passed through across the height of the sample, for which the internal heat conduction through the glass foam sample was around 662 mW. The internal heat flux was calculated with Fourier's law heat conduction equation based on the experimentally investigated temperatures across the glass foam thickness after the temperature plateau values were achieved [42]. Very similar trends of the temperature change over time were achieved after applying each layer of WO_3-based coating, indicating that the coating does not influence the thermal response of the glass foam. This can be explained based on the assumption that the extent of the optical response (in terms of reflected radiation) and the emissivity of the coating layering is insignificant to lead to a temperature modification considering the involved experimental conditions. When it comes to the thermal insulating properties of glass foam, it was highlighted, according to other experimental studies concerning the synthesis of glass foam from glass waste and to obtain valuable properties of interest, that the thermal conductivity depends on the porosity and compressive strength determined by the type of foaming agent, the raw materials and the synthesis conditions used for the glass.

Conclusion

We obtained dyed foam glass using a synthetic approach, which enables the production of high-efficiency, low-cost WO_3-based photochromic materials on a large scale with remarkable physical properties, flexible surface chemistry, thermal stability, and excellent biological properties like biocompatibility and nontoxic. Based on the optical investigation of the glass foam and of the applied layers of the WO_3-based coating, spectral reflectance of the coating increased from the 6.9% to 47% with the number of applied layers in the range between 480 and 580 nm corresponding to the yellow-green color, as visually detected. Moreover, the color change toward a green-blue color after solar irradiation given by the chromogenic properties of WO_3 can be considered an indicator of photon induced electron-hole pair mechanism that precedes also the photocatalysis phenomenon. These results make the coating attractive for further research activities in the photocatalytic field to develop new coatings with effects in pollution reduction.

The coating had no influence on the thermal response of the glass foam under direct simulated solar irradiation, so that the surface temperature and the temperature inside the glass foam reached approximately 80°C and respectively 74°C, 64°C, 51°C, 41°C (for T1, T2, T3, T4) before and after the application of the WO_3-based coating. The 3D scanning images illustrated the porous surface of the coated glass foam and a more appropriate application of the WO_3 based coating, free of cracks, after multiple layers, emphasized by the decrease in surface roughness. The FT-IR, Raman and XRD spectra led to the identification of carbon, the main functional groups of the commercial glass foam, especially Si-O and Si-O-Si, and of the monoclinic crystalline phase of the synthesized WO_3 pigment. Based on the EDAX analysis, other elemental components of the glass foam, Na, Ca, Mg and Al, were found additionally to those revealed in the FT-IR and Raman spectra.

Acknowledgment

This work was sustained within the project PN-III-P1-1.2-PCCDI-2017-0391/CIA_CLIM- "Smart buildings adaptable to the climate change effects" and the project PN-III-P2-2.1-PED-2019-2350, 322PED "Carbon dioxide methanizer design for sustainable low carbon energy systems development" and granted by Romanian Minister of Research and Innovation, CCCDI-UEFISCDI. S. F. Rus work was conducted within the PN-III-P1-1.1-MC-2019-1374 project granted by Romanian Minister of Research and Innovation, CCCDI-UEFISCDI.

Conflict of Interest

No conflict of interest.

Reference

1. Ya I Vaisman, AA Ketov, PA Ketov (2015) The scientific and technological aspects of foam glass production. Glass Phys Chem 41(2): 157-162.
2. Y Liu, J Xie, P Hao, Y Shi, Y Xu, et al. (2020) Study on Factors Affecting Properties of Foam Glass Made from Waste Glass. J Renew Mater 9(2): 237-253.
3. J Lu, K Onitsuka (2004) Construction utilization of foamed waste glass. J Environ Sci China 16(2): 302-307.
4. MJ Varady, AG Fedorov (2002) Combined Radiation and Conduction in Glass Foams. J Heat Transf 124(6): 1103-1109.
5. L Hu, F Bu, F Guo, Z Zhang (2017) Construction method of foam glass thermal insulation material in sloping roof. IOP Conf Ser Earth Environ Sci 61(1): 012122.
6. N Ghafari, P Segui, JP Bilodeau, J Côté, G Doré (2019) Assessment of mechanical and thermal properties of foam glass aggregates for use in pavements.
7. BA van Driel, SR van der Meer, KJ van den Berg, J Dik Determining (2019) The Presence of Photocatalytic Titanium White Pigments via Embedded Paint Sample Staining: A Proof of Principle. Stud Conserv 64(5): 261-272.
8. D Truffier-Boutry, B Fiorentino, V Bartolomei, R Soulas, O Sicardy, et al. (2017) Characterization of photocatalytic paints: a relationship between the photocatalytic properties – release of nanoparticles and volatile organic compounds. Environ Sci Nano 4(10): 1998-2009.
9. OL Evdokimova, TV Kusova, OS Ivanova, AB Shcherbakov, Kh E Yorov, et al. (2019) Highly reversible photochromism in composite WO_3/nanocellulose films. Cellulose 26(17): 9095-9105.
10. K Mouratis, Ioan Valentin Tudose, Cosmin Romanitan, Cristina Pachiu, Marian Popescu, et al. (2022) WO_3 Films Grown by Spray Pyrolysis for Smart Windows Applications. Coatings 12(4): 1-12.
11. R Vardhan, S Kumar, S Mandal (2020) A facile, low temperature spray pyrolysed tungsten oxide (WO_3): an approach to antifouling coating by amalgamating scratch resistant and water repellent properties. Bull Mater Sci 43: 281.

12. Guanyu Liu, Huiyun Xia, Yanhui Niu, Xu Zhao, Gengtong Zhang, et al. (2021) Fabrication of self-cleaning photocatalytic durable building coating based on WO_3-TNs/PDMS and NO degradation performance. Chem Eng J 409: 128187.

13. Y Zhen, BP Jelle, T Gao (2020) Electrochromic properties of WO_3 thin films: The role of film thickness. Anal Sci Adv 1(2): 124-131.

14. Xiaoni Li, Zhijie Li, Wanting He, Haolin Chen, Xiufeng Tang, et al. (2021) Enhanced Electrochromic Properties of Nanostructured WO_3 Film by Combination of Chemical and Physical Methods. Coatings 11(8): 959.

15. Gannian Zhang, Chung Man Ip, John Chow, Kahei Chan, Venus Lee, et al. (2020) Development of 7-Segment Numeral Display Using Electrochromic Yarns for Advanced Functional Textiles. J Text Sci Fash Technol 7(2): 1-7.

16. P Patnaik (2003) Handbook of inorganic chemicals. New York: McGraw-Hill.

17. S Wang, W Fan, Z Liu, A Yu, X Jiang (2018) Advances on tungsten oxide based photochromic materials: strategies to improve their photochromic properties. J Mater Chem C 6(2): 191-212.

18. D Nagy, D Nagy, IM Szilágyi, X Fan (2016) Effect of the morphology and phases of WO_3 nanocrystals on their photocatalytic efficiency. RSC Adv 6(40): 33743-33754.

19. Aminuddin Bin Ahmad Kayani, Sruthi Kuriakose,Mahta Monshipouri,Fararishah Abdul Khalid,Sumeet Walia et al. (2021) UV Photochromism in Transition Metal Oxides and Hybrid Materials. Small Weinh Bergstr Ger 17(32): e2100621.

20. J Jiang (2018) Advance of the Modified g-C_3N_4 Materials by Doping WO_x (X=0.1, 0.2, 0.3). Mod Concepts Mater Sci 1(1): 1.

21. Á Serrano-Aroca, S Deb (2020) Acrylate Polymers for Advanced Applications.

22. Paul Fazio, Hua Ge, Jiwu Rao, Guylaine Desmarais (2006) Research in Building Physics and Building Engineering: 3rd International Conference in Building Physics (Montreal, Canada, 27-31 August 2006). CRC Press, pp. 1008

23. E Carretti, L Dei (2004) Physicochemical characterization of acrylic polymeric resins coating porous materials of artistic interest. Prog Org Coat 49(3): 282-289.

24. HIS Nogueira, AMV Cavaleiro, J Rocha, T Trindade, JDP de Jesus (2004) Synthesis and characterization of tungsten trioxide powders prepared from tungstic acids. Mater Res Bull 39(4-5): 683-693.

25. MF Daniel, B Desbat, JC Lassegues, B Gerand, M Figlarz (1987) Infrared and Raman study of WO_3 tungsten trioxides and WO_3, xH2O tungsten trioxide tydrates. J Solid State Chem 67(2): 235-247.

26. N Prabhu, S Agilan, N Muthukumarasamy, CK Senthilkumaran (2013) Effect of temperature on the structural and optical properties of WO_3 nanoparticles prepared by solvo thermal method. Dig J Nanomater Biostructures 8(4): 1483-1490.

27. M Gotić, M Ivanda, S Popović, S Musić (2000) Synthesis of tungsten trioxide hydrates and their structural properties. Mater Sci Eng B 77(2): 193-201.

28. J Rajeswari, P Kishore, B Viswanathan, T Varadarajan (2007) Facile Hydrogen Evolution Reaction on WO_3 Nanorods. Nanoscale Res Lett 2(10): 496-503.

29. M Raja, J Chandrasekaran, M Balaji (2017) The Structural, Optical and Electrical Properties of Spin Coated WO_3 Thin Films Using Organic Acids. Silicon 9(2): 201-210.

30. Imre M Szilágyi, Balázs Fórizs, Olivier Rosseler, Ágnes Szegedie, Péter Németh, et al. (2012) WO_3 photocatalysts: Influence of structure and composition. J Catal 294: 119-127.

31. S Higashino, M Miyake, T Ikenoue, T Hirato (2019) Formation of a photocatalytic WO_3 surface layer on electrodeposited Al–W alloy coatings by selective dissolution and heat treatment. Sci Rep 9(1): 16008.

32. R Huang, Y Shen, L Zhao, M Yan (2012) Effect of hydrothermal temperature on structure and photochromic properties of WO_3 powder. Adv Powder Technol 23(2): 211-214.

33. VW Francis Thoo, N Zainuddin, KA Matori, SA Abdullah (2013) Studies on the Potential of Waste Soda Lime Silica Glass in Glass Ionomer Cement Production. Adv Mater Sci Eng 2013: e395012.

34. M Vilarigues, RC da Silva (2006) Characterization of potash-glass corrosion in aqueous solution by ion beam and IR spectroscopy. Journal of Non-Crystalline Solids 352(50-51): 5368-5375.

35. WB Stern, Y Gerber (2004) Potassium–Calcium Glass: New Data and Experiments. Archaeometry 46(1): 137-156.

36. L Bokobza, JL Bruneel, M Couzi Raman (2015) Spectra of Carbon-Based Materials (from Graphite to Carbon Black) and of Some Silicone Composites. C 1(1): 77-94.

37. AK Yadav, P Singh (2015) A review of the structures of oxide glasses by Raman spectroscopy. RSC Adv 5(83): 67583-67609.

38. S Bhowmick (2017) The RGB rendering of visible wavelength lights (2019 02 28 14 47 31 UTC).

39. Miguel A Arvizu, Hui-Ying Qu, Umut Cindemir, Zhen Qiu, Edgar A Rojas-González, et al. (2019) Electrochromic WO_3 thin films attain unprecedented durability by potentiostatic pretreatment. J Mater Chem A 7(6): 2908-2918.

40. Dong Yu Lu, Jian Chena, Huan Jun Chen, Li Gong, Shao Zhi Deng, et al. (2007) Raman study of thermochromic phase transition in tungsten trioxide nanowires. Appl Phys Lett 90(4): 041919.

41. A Mirzaei, JH Kim, HW Kim, SS Kim (2019) Gasochromic WO_3 Nanostructures for the Detection of Hydrogen Gas: An Overview. Appl Sci 9(9): 1775.

42. Charles H Forsberg (2021) Chapter 1 - Introduction to heat transfer. Heat Transfer Principles and Applications, pp. 1-21.